Age and petrogenesis of the Qassiarsuk carbonatite-alkaline silicate volcanic complex in the Gardar rift, South Greenland

TOM ANDERSEN

Laboratory of Isotope Geology, Mineralogical-Geological Museum, Sars gate 1, N-0562 Oslo, Norway

Abstract

The Qassiarsuk (formerly spelled Qagssiarssuk) complex is located in a roughly E–W trending graben structure between Qassiarsuk village and Tasiusaq settlement in the northern part of the Precambrian Gardar rift, South Greenland. The complex comprises a sequence of alkaline silicate tuffs and extrusive carbonatites interlayered with sandstones, and their subvolcanic equivalents, which represent possible feeders for the extrusive rocks. The Rb-Sr, Sm-Nd and Pb isotopic characteristics of 65 samples of extrusive carbonatite- and silicate tuffs and carbonatite diatremes have been determined by mass spectrometry. The Qassiarsuk complex can be dated to *c.* 1.2 Ga by Rb-Sr and Pb-Pb isochrons on whole-rocks and mineral separates, agreeing with previous isotopic ages for the volcanic rocks of the Eriksfjord formation in the Eriksfjord area of the Gardar rift, but not with previous, indirect age estimates of >1.31 Ga for assumed Eriksfjord equivalents in the Motzfeldt area further east. Recalculated isotopic compositions at 1.2 Ga indicate that the Qassiarsuk carbonatite- and alkaline-silicate magmas were comagmatic and derived from a depleted mantle source ($\varepsilon_{Nd}>4$, $\varepsilon_{Sr}<-13$, time-integrated, single- stage $^{238}U/^{204}Pb \leqslant 7.4$). The mantle-derived magmas were contaminated with crustal material, equivalent to the local, pre-Gardar granites and gneisses and sediments derived from these. The crustal component has a depleted mantle Nd model age of 2.1–2.6 Ga; at 1.2 Ga it was characterized by $\varepsilon_{Sr} = +76$, $\varepsilon_{Nd} = -8.4$, time-integrated, single- stage $^{238}U/^{204}Pb = 8.2–8.3$. Strong decoupling of the Pb from the Sr and Nd isotopic systems suggests that the contamination happened only after carbonatitic and alkaline-silicate magmas had evolved from a common parent, by processes such as liquid immisicibility and/or fractional crystallization. Post-magmatic hydrothermal alteration (oxidation, hydration of mafic silicates, carbonatization of melilite) may have contributed further to the contamination of the carbonatite and alkaline silicate rocks of the Qassiarsuk complex.

KEYWORDS: Gardar rift, Greenland, carbonatite, Rb-Sr, Sm-Nd, Pb-Pb.

Introduction

ALTHOUGH ultimately formed from mantle-derived parent magmas, carbonatites evolve by complex, and not always clearly understood processes. Mechanisms which have been suggested for the generation of carbonatite magma from a carbonate-bearing silicate parent magma include fractional crystallization, liquid immiscibility, and combinations thereof (e.g. Andersen, 1986, 1987, 1988; Church and Jones, 1995; Kjarsgaard and Hamilton, 1988, 1989; Le Bas, 1989; Peterson, 1989*a,b*, 1990). However, the relationship between a carbonatite and its mantle source may be obscured by element exchange with the country rocks, caused by contamination of the magma during ascent and crystallization (Andersen, 1987) or by post-magmatic, hydrothermal alteration processes (Andersen, 1983, 1984).

Radiogenic isotope data on carbonatites are useful both as potential indicators of mantle composition and -evolution (e.g. Bell and Blenkinsop, 1989; Kwon *et al.*, 1989) and as tracers of open-system processes in carbonatite magmas (e.g. Andersen, 1987). Especially for Precambrian carbonatites, the use of radiogenic isotope data to characterize petrogenic processes is complicated by the need to constrain the age of crystallization. Unfortunately, the poor resistance to surface weathering and some of the typical compositional characteristics of carbonatites make isotopic dating difficult. These include high Sr- and low Rb- concentration, high *REE* concentration levels, but little fractionation of Sm/Nd, and absence of good U-Pb mineral chronometers.

Mineralogical Magazine, August 1997, Vol. 61, pp. 499–513

Commonly, age determination is made on associated igneous silicate rocks, which are less troubled by such effects (e.g. Bruecner and Rex, 1980; Verschure *et al.*, 1983; Andersen and Sundvoll, 1986; Dahlgren, 1993). However, accumulation of apatite from phosphate-bearing carbonatite magmas cause considerable fractionation of U from Pb, making the mineral or whole-rock Pb-Pb system useful for direct dating of carbonatites (Andersen and Taylor, 1988; Jahn and Cuvellier, 1994; Andersen, 1996*a*).

Although one currently active carbonatite volcano is known (Oldoinyo Lengai, Tanzania; e.g. Dawson, 1962, 1989), extrusive carbonatites are less common through the geological record than their intrusive equivalents. The Qassiarsuk (formerly spelled Qagssiarssuk) complex in the Gardar Rift of South Greenland (Stewart, 1970), is an example which gives a unique opportunity to study well-preserved Precambrian extrusive and sub-volcanic carbonatites and their associated alkaline silicate rocks. Although parts of the Qassiarsuk complex were carefully mapped by Stewart (1970), the full areal extent of the carbonatites was recognized only during recent fieldwork (Andersen, 1996*b*). Stewart (1970) and Knudsen (1985) presented some major and trace element data from Qassiarsuk, but no radiogenic isotope data have so far been published. This paper presents the first Sr, Nd and Pb isotope data on the Qassiarsuk complex, constraining the age and petrogenesis of the carbonatites and their associated alkaline silicate rocks. A revised account of the geology, volcanic stratigraphy, petrography, geochemistry and petrology of the Qassiarsuk complex will be published separately (A.P. Jones and T. Andersen, work in preparation).

Geological setting

The volcanic and sub-volcanic rocks of the Qassiarsuk complex crop out within a roughly EW trending graben structure, extending from Qassiarsuk village on the Eriksfjord in the east to Tasiusaq inlet (Fig. 1), and possibly even to the North Sermilik fjord (west of the map limit in Fig. 1) in the west (Andersen unpublished field data). The well-known 'Qassiarsuk Triangle' described in detail by Stewart

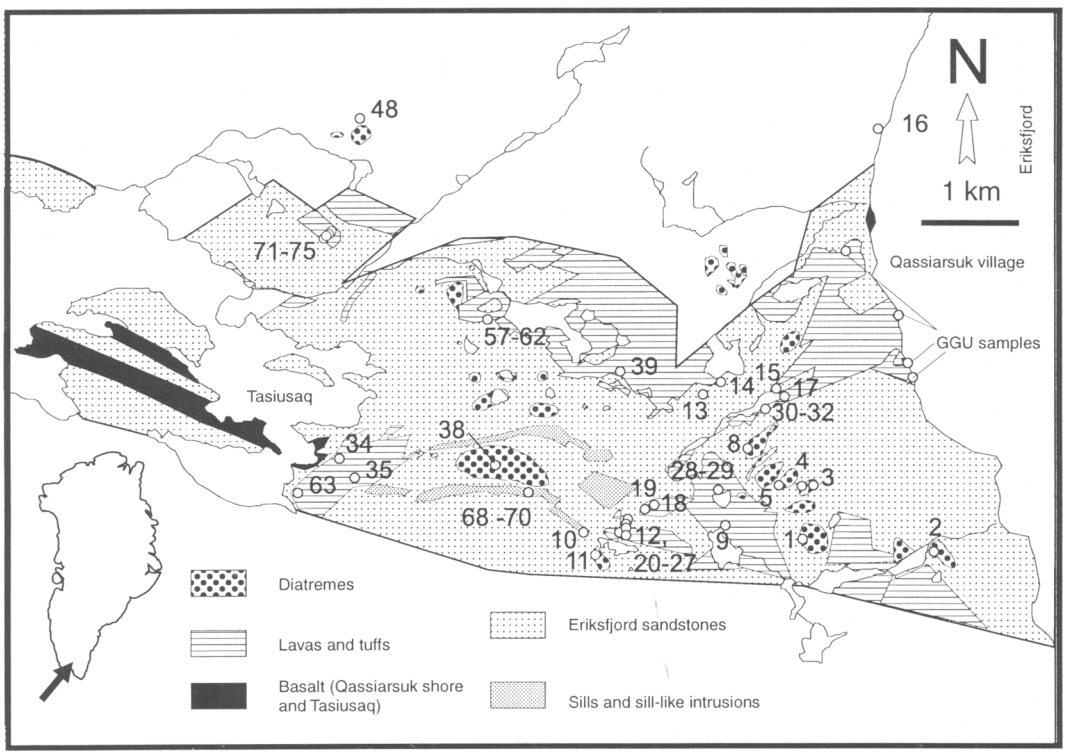

FIG. 1. Simplified geological map of the Qassiarsuk-Tasiusaq graben, Gardar Rift, S. Greenland, with localities of samples used in this study. Dykes and minor faults omitted. The pre-Gardar basement is left blank. Geological mapping by the present author, with some data from Stewart (1970) and A.P. Jones (pers. comm.)

(1970) makes up the easternmost part of this graben. The volcanic rocks of the Qassiarsuk complex have been equated with the the Mussartût volcanic Member of the Eriksfjord Formation (Poulsen, 1964; Emeleus and Upton, 1976; Allaart, 1983; Kalsbeek *et al.*, 1990); the sandstone below the volcanic rocks will then belong to the basal Majût sandstone Member (Allaart, 1983). The graben is limited against Ketilidian basement to the south by a prominent and continuous E–W 'master fault', and to the north by a zone of intersecting E–W and NE–SW faults. The entire area is penetrated by numerous doleritic to syenitic dykes trending close to N60°E, accompanied by minor faulting. Dyke injection and NE–SW faulting in general postdate the carbonatite volcanism, and probably also the subsidence of the E–W graben structure (A.P. Jones, personal communication).

The Qassiarsuk volcanic sequence is a well-defined unit within the sandstones, and can be mapped semi-continuously from Qassiarsuk at least as far west as the NW shore of Tasiusaq (formerly: Tasiussaq) inlet (Fig. 1). The thickness gradually decreases westwards, from *c.* 40 m in Qassiarsuk (Stewart, 1970) and in the central part of the graben to less than 10 m west of Tasiusaq. Thinner, discontinuous horizons of carbonatite tuff can be found above this main unit. An exaggerated estimate of a thickness of volcanic rocks of *c.* 375 m in the Qassiarsuk triangle was reported by Allaart (1983), but was probably influenced by unrecognized tectonic repetitions and by differences in dip between individual fault-blocks (Stewart, 1970).

A sequence of sandstones and interlayered igenous rocks of uncertain stratigraphic position crops out in the soutwestern part of the graben, SE of Tasiusaq. This area is separated from the rest of the graben by a prominent EW fault and contains a thick unit of carbonatite tuff, one large diatreme, and two major flat-lying intrusions, one of which is carbonatitic, the other doleritic.

Basaltic lavas cropping out in the east at the shore north of Qassiarsuk pier and in the west at the south shore of Tasiusaq inlet have not been studied in detail. The 'Qassiarsuk shore basalts' have an uncertain stratigraphic position (Stewart, 1970); the basalts at Tasiusaq are situated stratigraphically below the alkaline silicate and carbonatite tuffs of the SW segment of the graben (Andersen, unpublished field data).

The sandstones below the main volcanic sequence are penetrated by diatremes, which probably represent feeders for volcanic rocks. The diatremes range in composition from pure carbonatite through silicocarbonatite to melilitite/alnöite (Stewart, 1970) and trachyte-fonolite. A few alkaline silicate diatremes have been recognized within the Ketilidian basement north of the graben. Diatremes still further north (Stewart, 1970; Allaart, 1983) have not been investigated during the present study.

Material studied

The present study is based on samples collected by the author in 1992 and 1994, supplemented by samples from the collections of the Geological Survey of Denmark and Greenland, Copenhagen and Dr A.P. Jones, University College, London.

Carbonatites

The carbonatites range in composition from calcite carbonatite to iron-poor dolomite carbonatite and ankerite ferrocarbonatite. In terms of microstructure, massive, globular and laminated varieties can be distinguished. The massive carbonatites consist of coarse-grained sparry carbonate, enclosing totally oxidized pseudomorphs after mafic silicates, which today are composed of hematite, chlorite and serpentine. No primary igneous textures can be identified. This rock type has many textural and mineralogical features in common with the 'rødberg' ('red-rock') from the Fen complex, Norway (Andersen, 1984), and has probably formed by similar processes, i.e. by post-magmatic alteration of pre-existing carbonatite. In some of the samples, calcite has most probably replaced melilite and/or alkali feldspar, as shown by the existence of multi-grain pseudomorphs which have preserved the outlines of the primary minerals and which contain occasional relics of silicates.

The laminated carbonatites consist of well-preserved plate-shaped carbonate crystals, building up a flow-laminated microstructure. The carbonate crystals of the laminated carbonatite differ from the pseudomorphs after silicate minerals in consisting of a single, optically continous calcite crystal.

The globular carbonatite is found both as an extrusive rock (the lapilli-tuff of Stewart, 1970) and in diatremes. The rock is built up from millimetre-sized pellets consisting of platy carbonate crystals set in a fine-grained, opaque to semi-opaque matrix. The groundmass consists of anhedral, sparry carbonate, mixed with sand-sized, well-rounded grains of quartz. Some of the samples also contain pellets of silicate material; a gradual transition between carbonatite and alkaline silicate end-members may possibly exist.

Stewart (1970) used the presence of platy carbonate crystals as an indication that the carbonate had formed by replacement of melilite. Although this can clearly be observed in some samples, the textural argument for the former presence of melilite is not valid in general, as both a platy carbonate mineral habit and

flow-laminated microstructures are common in carbonatites of undisputed volcanic or primary intrusive origin (e.g. Barker, 1989; Keller, 1989).

Alkaline silicate rocks

The alkaline silicate rocks which have been examined in this study are melilitites with or without relict olivine, alnöitic lamprophyres, containing primary mica in addition to melilite, pyroxene and olivine (Stewart, 1970) and tuffs of trachytic to phonolitic composition. In the diatremes and minor sub-volcanic intrusions/feeder pipes massive and globular varieties are found. The massive melilitite consists of euhedral melilite laths, with a strongly altered, fine-grained interstitial material. The globular variety and the melilitic tuff contains lapilli consisting of melilite-laths set in a fine-grained, opaque or semi-opaque matrix. The groundmass consists of strongly altered silicate material with minor amounts of carbonate. The melilite is always partly replaced by carbonate.The trachytic-phonolitic tuff contains lapilli of nearly opaque devitrified glass with euhedral phenocryst of potassium feldspar, set in a groundmass of detritial quartz grains cemented by devitrified glass.

Micas for Rb-Sr mineral dating were separated from five samples of alnöitic lamprophyre selected from the collection of Dr A.P. Jones. These samples were crushed manually in a steel percussion mortar to sub-millimetre size, and flakes of mica were separated by hand-picking.

Apatite-rich rocks

The apatite-rich samples used in the present study were selected from a suite of phosphorus rich rocks from the Qassiarsuk Triangle studied by Knudsen (1985), and comprise carbonatite lavas and tuffs, and an apatite-rich facies from an alnöitic lamprophyre intrusion. The samples were provided by the Geological Survey of Denmark and Greenland (GEUS), Copenhagen. Whole-rock P_2O_5 contents range from 3 to 35 weight percent (Table 1, data from Knudsen, 1985, Table 7).

Country rocks

To evaluate the influence of the local country rocks on the isotopic systems of the Qassiarsuk igneous rocks, three composite country-rock samples were collected. GRAN is a composite of granitic rocks, collected along the trail from Qassiarsuk to Tasiusaq, in the basement north of the graben structure. QSS is a composite of the sandstone immediately below the volcanic rocks, collected at Qassiarsuk village, whereas TSS is a composite of sandstones above the main tuff sequence, collected in the Tasiusaq area. Sample 48 is a slightly metasomatized granitic gneiss ('fenite') collected near the contact to a diatreme NW of Tasiusaq.

Radiogenic isotope geochemistry

Analytical methods

Rb, Sr, Sm, Nd and Pb were separated from finely crushed and homogenized whole-rock powders and from hand-picked mineral separates by standard ion exchange procedures. Sr, Nd and Pb isotopic ratios were determined by mass spectrometry, using a fully automated Finnigan MAT 262 mass spectrometer in the Laboratory of Isotope Geology, Mineralogical-Geological Museum, Oslo. Nd isotopic compositions are normalized to $^{146}Nd/^{144}Nd = 0.7219$. During the period the present analyses were made, the Johnson and Matthey batch no. S819093A Nd_2O_3 gave $^{143}Nd/^{144}Nd = 0.511101 \pm 0.000013$. The NBS 987 Sr standard yielded $^{87}Sr/^{86}Sr = 0.710228 \pm 0.000050$. The isotopic composition of lead was determined using the phosphoric acid-silica gel method on single rhenium filaments. Lead isotope ratios were corrected for mass fractionation off-line, using a correction factor of 0.095 %/AMU derived from multiple runs of the NBS SRM 981 common lead standard (composition from Todt *et al.*, 1984). Rb, Sr, Sm and Nd concentrations were determined by isotope dilution, using aliqots spiked in ^{87}Rb, ^{84}Sr, ^{149}Sm and ^{148}Nd or ^{150} Nd. A VG354 mass spectrometer was used for the isotope dilution analyses.

Isochron calculations have been made using the Isoplot 2.57 software package (Ludwig, 1991), multi-stage lead modelling and other calculations by interactive spreadsheet programs written by the present author. For age calculation of poorly-fitted isochrons with elevated MSWD, models 2 and 3 of Ludwig (1991) were used, which include estimates of initial isotopic heterogeneity in the isochron calculation. Lead isotopes are discussed in terms of a two-stage model of global lead evolution (e.g. Faure, 1977), identical to that used by Andersen and Munz (1995). In this model, the age of the Earth = 4.57 Ga, and lead has evolved from an initial meteoritic composition (Tatsumoto *et al.*, 1973) in a reservoir with a time-integrated $^{238}U/^{204}Pb$, given as the μ_1 of a single sample or the single-stage model μ calculated for a lead isochron, until formation of the Qassiarsuk complex at t. Lead was then extracted from different sub-reservoirs, and the samples evolved in individual, closed and homogeneous systems with constant $^{238}U/^{204}Pb$ (μ_2) until the present. When t is given, each sample is characterized by unique μ_1 and μ_2 values.

Trace element concentrations

The trace element geochemisty of the Qassiarsuk complex will be the subject of a separate study (Jones and Andersen in prep.). In this paper, only the trace element concentrations determined by isotope dilution as part of the radiogenic isotope study will be considered. The carbonatites and the apatite-rich rocks are characterized by high strontium contents (570 to 3800 ppm) coupled with Rb concentrations below 200 ppm. The *REE* contents are variable (40 to 750 ppm Nd), and the samples are enriched in light relative to heavy *REE*, expressed by a f_{Sm} value for individual samples $\{f_{Sm} = (^{147}Sm/^{143}Nd)_{Sample}/(^{147}Sm/^{144}Nd)_{CHUR} - 1\} \leqslant -0.3$. The alkaline silicate rocks have lower *REE* concentrations (< 150 ppm Nd), lower Sr (< 1800 ppm) but comparable Rb concentrations. The Sr and Nd concentrations and the degree of relative *LREE* enrichment (expressed by $-1 < f_{Sm} < 0$) are correlated along single trends (Fig. 2*a,b*). Although the alkaline silicate rocks and the carbonatites plot at opposite ends of these trends, there is moderate overlap between the two groups, and there is thus no gap in trace element concentrations between the alkaline silicate rocks and the carbonatites.

The rubidium-strontium system

Whole-rocks. The carbonatites are characterized by low $^{87}Rb/^{86}Sr$, whereas the $^{87}Rb/^{86}Sr$ of the alkaline silicate rocks ranges from near zero to 2.5 (Table 1, Fig. 3). A regression of all silicate tuffs together results in a very poorly fitted correlation line (MSWD = *c.* 300), with an indication of an age of 1221 ± 19 Ma and an initial ratio of 0.7031. Time-corrected $^{87}Sr/^{86}Sr$ ratios at 1.2 Ga show considerable spread (0.70493 to 0.70272; i.e. $\varepsilon_{Sr} = +24$ to -12.8), indicating that the magma was indeed heterogeneous at the time of crystallization. The most likely reason for the initial strontium isotopic heterogeneity is crustal contamination, leading to a general increase of $^{87}Sr/^{86}Sr$ in samples which have been affected. To minimize the effect of contamination on the Rb-Sr system, a 7-point isochron was calculated for samples having $^{87}Sr/^{86}Sr \leqslant 0.7030$ at 1.2 Ga. This gave a moderately well-fitted isochron (MSWD = 2.94) with an age of 1205 ± 12 Ma and an initial ratio of 0.7029 (Fig. 2). Most samples plot above this line, including many of the carbonatites, suggesting that contamination processes may have influenced even Sr-rich carbonatite magma.

The granite composite and the 'fenitized' granitic gneiss (sample 48) show uniform $^{87}Sr/^{86}Sr$ of 0.7086 ($\varepsilon_{Sr} = +76$) at 1.2 Ga, which is typical of a moderately LILE-enriched Precambrian crustal rock composition. Syn-intrusive metasomatism has not affected the Sr isotope system of the 'fenite'. The two sandstone composite samples and one of the carbonatite diatremes have unrealistically low time-corrected $^{87}Sr/^{86}Sr$ ratios (0.6976 and 0.7015), and are probably influenced by loss of radiogenic strontium by recent surface weathering.

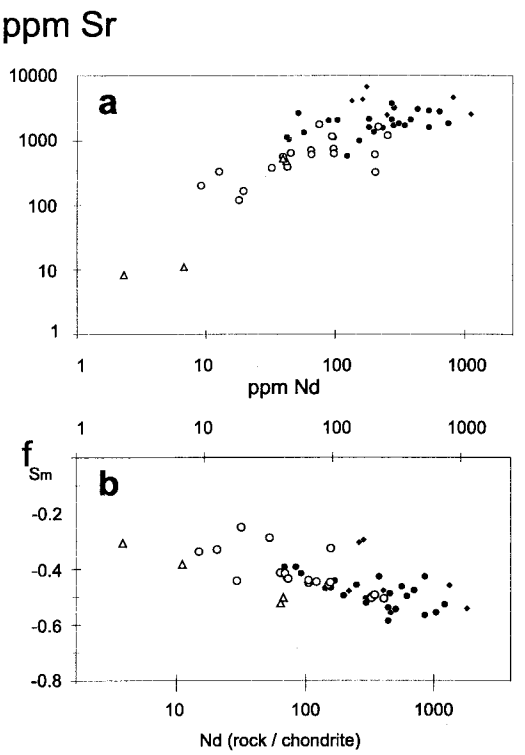

FIG. 2. Correlation between (a) Sr and Nd concentrations, and (b) between Nd concentration and Sm enrichment factor for individual samples. The lower scale gives Nd concentrations relative to a chondritic value of 0.60 ppm (Boynton, 1984). The samarium-enrichment factor relative to chondrites is defined by: $f_{Sm}=(^{147}Sm/^{143}Nd)_{Sample}/(^{147}Sm/^{144}Nd)_{CHUR} - 1$. Sample signatures: Solid circles: Carbonatites. Solid diamond: Apatite-rich carbonatites and lamprophyres. Open circles: Alkaline silicate rocks. Triangles: Country rocks.

Mica separates. Four of the five phlogopite separates from alnöitic lamprophyre intrusions plot along an imperfectly fitted regression line (MSWD = 23) with a date of 1234 ± 34 Ma and an intitial ratio of 0.7043 ± 0.0004 (Table 1, Fig. 4). This date is indistinguishable from that of the whole-rock line, but the corresponding initial ratio is significantly higher. One phlogopite separate plots well above this regression line. The Rb-Sr systematics of the micas

TABLE 1. Radiogenic isotope data from the Qassiarsuk complex

Sample		Sm ppm	Nd ppm	$^{147}Sm/^{144}Nd$	$^{143}Nd/^{144}Nd$	2σ	Rb ppm	Sr ppm	$^{87}Rb/^{86}Sr$	$^{87}Sr/^{86}Sr$	2σ	$^{206}Pb/^{204}Pb$	2σ	$^{207}Pb/^{204}Pb$	2σ	$^{208}Pb/^{204}Pb$	2σ
Carbonatite																	
92/1	Diatreme	41	286	0.0881	0.511834	0.000010	176	3236	0.158	0.705530	0.000030	17.000	0.017	15.264	0.015	40.356	0.040
92/2	Diatreme	29	184	0.0973	0.511996	0.000010	1.2	2149	0.002	0.703217	0.000030	16.389	0.016	15.252	0.015	38.822	0.039
92/3	Diatreme	27	154	0.1068	0.512091	0.000010	2.0	996	0.006	0.703471	0.000030	20.032	0.020	15.557	0.016	40.879	0.041
92/4	Diatreme	37	273	0.0817	0.511888	0.000010	0.8	2121	0.001	0.703275	0.000030	16.445	0.016	15.278	0.015	36.340	0.036
92/5	Diatreme	28	184	0.0943	0.511877	0.000010	2.7	1625	0.005	0.703319	0.000030	17.008	0.017	15.320	0.015	40.437	0.040
92/6	Diatreme	47	281	0.1011	0.511980	0.000010	2.0	1733	0.003	0.703503	0.000030	16.572	0.017	15.289	0.015	36.293	0.036
92/7	Diatreme	92	640	0.0874	0.511877	0.000010	1.8	2785	0.002	0.703941	0.000030	16.466	0.016	15.219	0.015	40.740	0.041
92/8	Diatreme	46	312	0.0896	0.511877	0.000010	67	1864	0.105	0.703342	0.000030	16.457	0.016	15.262	0.015	38.385	0.038
92/9	Tuff	33	200	0.0990	0.511877	0.000010	1.5	1371	0.003	0.704990	0.000030	17.544	0.018	15.307	0.015	40.154	0.040
92/10	Dyke						0.8	3308	0.001	0.702901	0.000030	16.653	0.017	15.274	0.015	38.247	0.038
92/11	Diatreme	62	381	0.0992	0.511905	0.000010	5.1	2116	0.007	0.703274	0.000030	16.337	0.025	15.224	0.021	39.213	0.060
92/12	Dyke	8.0	44	0.1117	0.512108	0.000010	109	1056	0.299	0.708100	0.000030						
92/13	Dyke	98	526	0.1130	0.511204	0.000010	7.5	1616	0.013	0.704070	0.000030	17.174	0.017	15.294	0.015	42.262	0.042
92/14	Dyke						111	893	0.361	0.709278	0.000030	16.845	0.017	15.277	0.015	37.032	0.037
92/15	Dyke						20	2318	0.025	0.703627	0.000030	16.970	0.017	15.323	0.015	39.828	0.040
92/16	Dyke	73	433	0.1031	0.511877	0.000010	1.4	3072	0.001	0.703407	0.000030	20.392	0.020	15.641	0.016	42.395	0.042
92/24	Tuff	10.1	52	0.1198	0.512107	0.000010	93	2670	0.102	0.704833	0.000030	18.754	0.019	15.401	0.015	37.573	0.037
92/25	Tuff						1.6	3831	0.001	0.703106	0.000030	16.518	0.016	15.245	0.015	51.416	0.051
92/26	Tuff	8.3	42	0.1198	0.512086	0.000010	109	1137	0.277	0.707881	0.000030						
92/27	Tuff	10.8	57	0.1153	0.512088	0.000010	33	1349	0.072	0.704661	0.000030	18.138	0.018	15.223	0.015	38.500	0.038
94/63	Tuff	41	273	0.0907	0.511984	0.000010	0.6	3749	0.000	0.702973	0.000030	16.338	0.016	15.330	0.015	36.736	0.037
94/73	Tuff	15	89	0.1047	0.511964	0.000010	31	2072	0.043	0.705084	0.000030	18.747	0.019	15.494	0.015	38.981	0.039
94/74	Tuff	20	123	0.0993	0.511978	0.000010	0.5	573	0.002	0.704203	0.000030	82.039	0.138	20.642	0.035	40.869	0.084
94/34	Tuff	114	748	0.0930	0.512000	0.000013	17.5	1842	0.028	0.703369	0.000030						
94/35	Tuff	43	232	0.1130	0.512130	0.000010	0.3	1600	0.001	0.703775	0.000030						
94/38	Diatreme	74	525	0.0857	0.511919	0.000024	1.9	2898	0.002	0.702834	0.000030						
94/39	Tuff	17	98	0.1051	0.511939	0.000007	125	1116	0.324	0.708427	0.000030						
94/40	Tuff	60	346	0.1060	0.512066	0.000010	1.2	1734	0.002	0.703690	0.000030						
94/57	Tuff	19	104	0.1098	0.512048	0.000010	83	2100	0.115	0.704914	0.000030						
Apatite-rich carbonatites and lamprophyres																	
	wt% P_2O_5																
GGU 320209	3.81	23	135	0.1026	0.511983	0.000010	32	4114	0.023	0.703621	0.000030	22.087	0.039	15.683	0.027	37.211	0.072
GGU 320211	3.12	42	251	0.1029	0.512020	0.000015	51	2471	0.060	0.703849	0.000030	22.747	0.038	15.718	0.027	41.202	0.103
GGU 320231	35.18	40	175	0.1386	0.512310	0.000010	150	6775	0.064	0.703447	0.000030	150.465	0.171	25.813	0.029	42.991	0.075
GGU 320232		37	163	0.1369	0.512213	0.000010	34	4296	0.023	0.704596	0.000030	164.776	0.176	26.939	0.029	44.326	0.050
GGU 320244		143	815	0.1067	0.512019	0.000200	14	4597	0.009	0.704633	0.000030	155.306	2.131	26.413	0.364	40.134	0.579
GGU 320247												20.095	0.002	15.397	0.001	53.083	0.006
GGU 320257	20.23						1.3	7779	0.000	0.702780	0.000030	17.469	0.003	15.287	0.003	36.588	0.054
GGU 320258							20	2010	0.029	0.703218	0.000030	16.390	0.002	15.196	0.002	46.349	0.016

TABLE 1. (*contd.*)

Sample		Sm ppm	Nd ppm	$^{147}Sm/^{144}Nd$	$^{143}Nd/^{144}Nd$	2σ	Rb ppm	Sr ppm	$^{87}Rb/^{86}Sr$	$^{87}Sr/^{86}Sr$	2σ	$^{206}Pb/^{204}Pb$	2σ	$^{207}Pb/^{204}Pb$	2σ	$^{208}Pb/^{204}Pb$	2σ
Alkaline silicate rocks																	
92/17	Tuff						92.1	574	0.466	0.712380	0.000030	18.948	0.019	15.314	0.015	38.503	0.038
92/18	Tuff	2.0	9.1	0.1306	0.512010	0.000010	163.6	200	2.389	0.745430	0.000030	17.592	0.021	15.294	0.018	37.053	0.042
92/19	Tuff	7.4	32	0.1402	0.511877	0.000010	130.2	376	1.007	0.720650	0.000030	16.192	0.016	15.016	0.015	37.545	0.037
92/20	Tuff	4.7	20	0.1478	0.512097	0.000010	90.5	165	1.594	0.731313	0.000030						
92/21	Tuff	13.5	75	0.1093	0.512048	0.000010	105.6	1795	0.171	0.705809	0.000030						
92/22	Tuff	2.7	12.6	0.1319	0.512082	0.000010	74.5	328	0.661	0.715358	0.000030						
92/23	Tuff	12	65	0.1083	0.512040	0.000010	85	708	0.348	0.708870	0.000030						
92/28	Tuff	7.4	39	0.1155	0.512044	0.000010	92	561	0.476	0.711540	0.000030	21.660	0.022	15.567	0.016	39.033	0.039
92/29	Tuff	8.0	43	0.1150	0.512037	0.000010	75	386	0.569	0.713070	0.000030						
92/30	Tuff	3.2	18	0.1099	0.511912	0.000010	33	119	0.797	0.716665	0.000030						
92/31	Tuff	8.3	45	0.1115	0.512039	0.000010	49	645	0.222	0.707963	0.000400	22.154	0.022	15.599	0.016	41.754	0.042
92/32	Tuff	12	65	0.1102	0.512037	0.000010	53	603	0.255	0.707305	0.000030						
94/58	Tuff	33	205	0.0980	0.511900	0.000013	133	323	1.196	0.723809	0.000030						
94/59	Tuff	40	254	0.0971	0.511894	0.000010	129	1209	0.308	0.708373	0.000030						
94/61	Tuff	17	94	0.1071	0.511991	0.000010											
94/62	Tuff	17	97	0.1090	0.512033	0.000010	75	750	0.288	0.708055	0.000030	23.107	0.023	15.752	0.017	45.187	0.056
94/68	Sill	33	203	0.0977	0.512000	0.000010	7.2	604	0.035	0.703803	0.000030	16.766	0.017	15.430	0.021	37.010	0.068
94/70	Sill	35	215	0.0997	0.512040	0.000010	50	1642	0.088	0.704454	0.000030						
94/72	Tuff	21	98	0.1329	0.512176	0.000010	127	628	0.586	0.713147	0.000030	18.694	0.019	15.525	0.016	37.942	0.038
288311	Mica						757	223	10.03	0.883067	0.000030						
288339A	Mica						477	516	2.70	0.752095	0.000030						
288341B	Mica						316	225	4.09	0.775634	0.000030						
288412	Mica						173	3580	0.14	0.706827	0.000030						
345	Mica						413	113	10.87	0.934577	0.000030						
Country rocks																	
GRAN	Granite composite	6.8	42	0.0979	0.511409	0.000014	179	474	1.093	0.727385	0.000030	21.809	0.022	15.914	0.016	39.295	0.039
TA94/48	'Fenite'	6.1	39	0.0940	0.511418	0.000010	268	517	1.504	0.734400	0.000030						
SSQ	Sandstone composite	0.5	2.3	0.1365	0.511708	0.000103	12.9	8.3	4.542	0.778590	0.000032	23.233	0.122	16.021	0.088	39.024	0.210
SST	"	1.4	6.8	0.1217	0.511649	0.000017	14.6	10.9	3.871	0.764094	0.000030	19.856	0.224	15.817	0.176	39.230	0.440

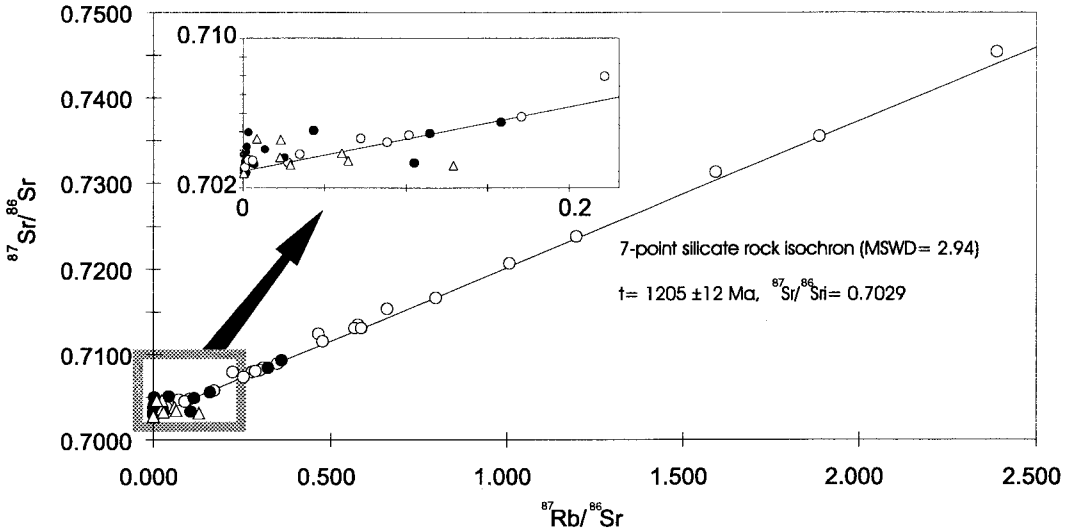

FIG. 3. Rb-Sr isochron diagram. The 'Silicate rock isochron' has been calculated from 7 samples of silicate tuff, whose $^{87}Sr/^{86}Sr$ ratio at 1.2 Ga $\leqslant$ 0.7030. Three points falling below this isochron (the two sandstone composites and carbonatite 92/8) have unrealistically low $^{87}Sr/^{86}Sr$ at 1.2 Ga (< 0.702), and have probably lost radiogenic strontium by recent surface weathering. Sample symbols as in Fig. 2.

from lamprophyres indicate crystallization from melts with elevated and heterogeneous strontium isotopic composition, most likely caused by variable crustal contamination of a low-$^{87}Sr/^{86}Sr$ mantle-derived magma. The Qassiarsuk lamprophyre micas are thus unlike the phlogopites from damtjernite in the Fen complex, Norway, which show only moderate differences in initial $^{87}Sr/^{86}Sr$ between individual intrusions, allowing the igneous complex to be dated by a composite mica Rb-Sr isochron (Dahlgren, 1987, 1993).

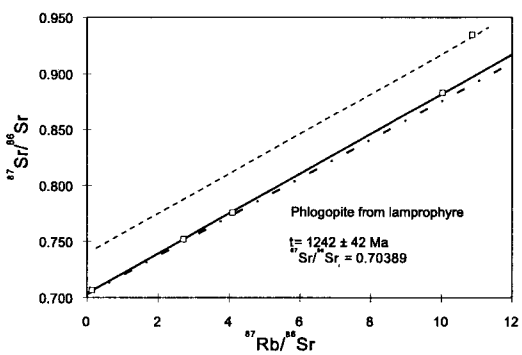

FIG. 4. Rb-Sr isochron diagram for mica separates from alnöitic lamprophyres. Solid line: 4-point isochron for mica separates. Dash-dot line: Silicate rock isochron, from Fig. 2. Dotted line: Reference isochron for a contaminated lamprophyre.

The lead isotope system

Like their counterparts in several other carbonatite complexes, the Qassiarsuk carbonatites and associated apatite-rich rocks show a large spread of the U/Pb ratio, probably caused by differentiation during crystallization of apatite and calcite from carbonatite magma (Andersen and Taylor, 1988). The resulting spread in present-day $^{206}Pb/^{204}Pb$ from *c.* 16.3 to 155 (Table 1, Fig. 5) is of the same order of magnitude as the variation in the Fen and Alnö carbonatites (Andersen and Taylor, 1988; Andersen, 1996*a*). When all carbonatites and apatite-rich rocks are regressed together, an imperfectly fitted line (MSWD = 29) is obtained, with an age of 1182 $\pm$ 19 Ma (Model 2 age, Ludwig, 1991). When only six of the apatite-rich rocks are included, the fit is significantly improved (MSWD = 4.4), but the age remains unchanged (1176 $\pm$ 8 Ma, Model 1 of Ludwig, 1991). The single-stage model-μ of this regression line is 7.77. The three composite country-rock samples plot well above this line, along a generally parallel trend (Fig. 5*b*).

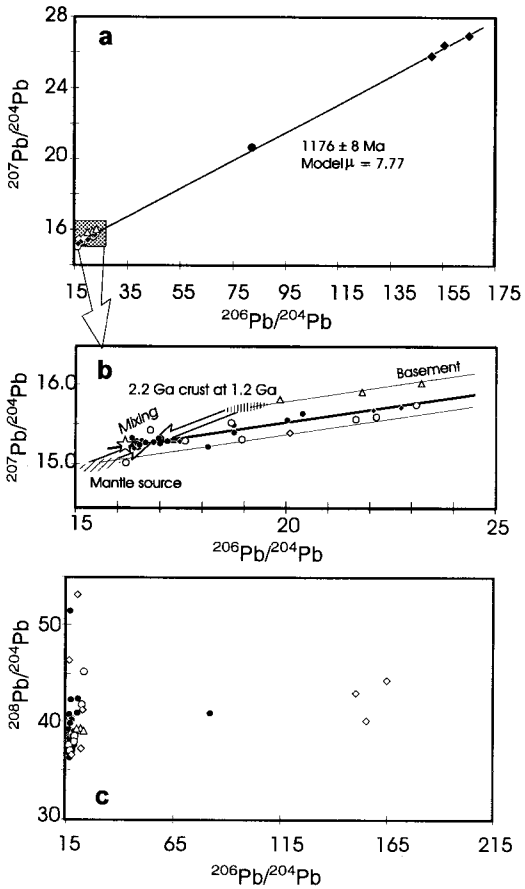

FIG. 5. Pb-Pb systematics of the Qassiarsuk rocks. Sample signatures as in Fig. 2. (*a*): Uranogenic lead correlation diagram. The isochron is based on 6 samples of apatite-rich carbonatite and lamprophyre. (*b*): Detail of *a*, showing the carbonatite isochron (heavy, from *a*). Ranges of variation for 2.2 Ga continental crust (vertical ruling), representing the local crustal contaminant, and of a 1.2 Ga mantle-source with $\mu_1 = 7.4$ (diagonal ruling) are shown, with a possible mixing line between the two components (opposing arrows), which would produce initial lead isotopic composition of the main group of samples ($\mu_1 \geqslant 7.7$). The samples falling significantly below this line cannot have experienced much contamination during ascent through the crust and by post-magmatic alteration. The star indicates the preferred composition of the mantle source for the Tugtutôq younger giant dyke and the Kûngnât Fjeld intrusion (Taylor and Upton, 1993). *c*: Thorogenic lead correlation diagram, showing lack of linear correlation of thorogenic and uranogenic lead, due to significant fractionation of U from Th during formation of the Qassiarsuk complex.

The alkaline silicate rocks show more 'unsupported' scatter of $^{207}Pb/^{204}Pb$ than the carbonatites, at generally less radiogenic compositions ($^{206}Pb/^{204}Pb < 23.1$). Points scattering above the carbonatite-apatite rock line can be explained by crustal contamination, but the points falling distinctly below the line must be due to other processes. A group of samples, including sample 19 (silicate tuff), which is uncommonly unradiogenic in the uranogenic lead isotopes ($^{206}Pb/^{204}Pb = 16.192$, $^{207}Pb/^{204}Pb = 15.016$), plot close to a reference isochron with model-μ of 7.4–7.5, which must reflect a much less radiogenic initial lead than the samples on the main correlation line.

The variation in thorogenic lead is considerable, though less extreme than in uranogenic lead, with $^{208}Pb/^{204}Pb$ from 35 to above 50 (Fig. 5*c*). The relative variation is largest among the apatite-rich rocks and the carbonatites, and it is uncorrelated with the $^{206}Pb/^{204}Pb$ ratio. This merely reflects fractionation of the U/Th ratio during crystallization of the carbonatite magma, and does not have any geochronological consequences, contrary to what was suggested by Dahlgren (1993).

The samarium-neodymium system

The carbonatites and alkaline silicate rocks show restricted and overlapping ranges of $^{147}Sm/^{144}Nd$ (0.082–0.148; Table 1). Recalculated $^{143}Nd/^{144}Nd$ at 1.2 Ga ranges from 0.51127 ($\varepsilon_{Nd} = +3.6$) to 0.51077 ($\varepsilon_{Nd} = -6.2$). This can be compared to initial Nd isotopic compositions of 0.51121 ± 1 ($\varepsilon_{Nd} = +2.4$) for 1.17–1.20 Ga lavas from the Ulukasik Member of the Eriksfjord Formation reported by Paslick *et al.* (1993).

The granitic country rock composites, the sample of 'fenite' from Tasiusaq (sample 48) and the two sandstone composites show rather uniform Nd isotopic compositions at 1.2 Ga, with $^{144}Nd/^{144}Nd = 0.51063$ to 0.51069 ($\varepsilon_{Nd} = -8.9$ to -7.8). This can be recalculated to depleted mantle model ages (De Paolo, 1981 -model) of 2.1–2.6 Ga, suggesting that the local crustal protolith dates back to the early Proterozoic, and that the sandstones have been derived from a source comparable to the underlying granite.

Discussion

The age of the Qassiarsuk volcanic sequence, and its regional significance

The three isochron ages determined for minerals and rocks from the Qassiarsuk complex all fall close to 1.2 Ga, with variable uncertainty and quality of fit.

Crustal contamination has certainly caused heterogeneity in the initial strontium composition which, due to the restricted spread in Rb/Sr ratio, has not been overshadowed by accumulated radiogenic strontium. By limiting the time-corrected $^{87}Sr/^{86}Sr$ at 1.2 Ga to less than a certain value (0.7030), and rejecting all samples falling above this limit as contaminated, a better isochron, which is less influenced by crustal contamination, is obtained (1205 $\pm$ 12 Ma). It should, however, be noted that this age-estimate is based on a boundary condition (the limit of 1.2 Ga recalculated strontium composition) which is somewhat arbitrary and lacking in geological justification.

The lead isotopic system of the Qassiarsuk carbonatites is also affected by crustal contamination, leading to scatter around the Pb-Pb isochron. The regression lines calculated for these rocks correspond to a special case of U-Pb scenario 2a of Whitehouse (1989), in which a meaningful age may be obtained despite poor initial isotopic homogenization, because the initial isotopic heterogeneity is totally overshadowed by accumulated radiogenic lead. The isochron calculated for the apatite-rich rocks alone (1176 $\pm$ 8 Ma) gives the best fit, and is regarded as the best estimate of the age of the Qassiarsuk carbonatite.

This age of the Qassiarsuk complex (and thereby of the Mussartût volcanic Member of the Eriksfjord Formation) is indistinguishable within uncertainty from Nd mineral isochron ages of 1.17 $\pm$ 0.03 Ga and 1.20 $\pm$ 0.03 Ga obtained for mafic lavas of the overlying Ulukasik volcanic Member by Paslick *et al.* (1993). This suggests that deposition of the Eriksfjord sandstones and volcanic rocks has been a comparatively rapid process, with deposition of a large proportion of the entire succession taking place within the age resolution of the dating methods used (i.e. within 8 to 30 Ma). Deposition of the Eriksfjord Formation within such a short period of time is in conflict with the observation that lavas and sediments correlated with the Eriksfjord Formation are cross-cut by intrusions belonging to the 1.31-1.35 Ga Motzfeldt centre of the Igaliko complex (Blaxland *et al.*, 1978; Allaart, 1983, Paslick *et al.*, 1993; Kalsbeek *et al.*, 1990), which suggest an onset of volcanism and sedimentation more than 100 Ma before the formation of the Qassiarsuk complex. If the assumption of 1.31 - 1.35 Ga Eriksfjord-equivalents in the area NE of Motzfeldt is correct, it implies that the tectonomagmatic evolution of the Gardar rift may be more complex than previously assumed, with distinct periods of volcanism in the Motzfeldt area and in the area west of Eriksfjord. Alternatively, the intrusions cross-cutting the Eriksfjord-Formation equivalents at Motzfeldt may be younger than the 1.31- 1.35 Ga rocks dated by Blaxland *et al.* (1978) and Paslick *et al.* (1993).

Petrogenesis of the Eriksfjord magmas

The present radiogenic isotopic study cannot identify the actual processes by which magma formed and evolved into carbonatite and alkaline silicate fractions at Qassiarsuk. However, the observations that both end-member components (i.e. carbonatite and alkaline silicate rocks) fall on continuous trace element trends (Fig. 2), and that the most 'primitive' initial radiogenic isotope compositions in each group overlap (Figs. 3, 5) suggest that they are indeed comagmatic, and that the carbonatite magma may have formed from a carbonate-bearing silicate parent magma by processes such as fractional crystallization or liquid immiscibility. The source region in the mantle has a clear depleted mantle signature (i.e. $\varepsilon_{Nd} > 0$, $\varepsilon_{Sr} < 0$, single-stage $\mu < 8$), as is the case with most carbonatites throughout the geological record (see reviews by Bell and Blenkinsop, 1989 and Kwon *et al.*, 1989). Producing magmas which are enriched in CO_2 and *LREE* from a depleted mantle source requires some pre-melting metasomatic re-enrichment of the mantle source in these components, which may be a general process in the generation of carbonatites and related igneous rocks (e.g. Andersen, 1987).

Crustal contamination vs. mantle heterogeneity

The variation in initial Sr, Nd and Pb isotopic signature can in principle be caused by two processes: (1): Melting of a heterogeneous mantle source, followed by imperfect homogenization of the magma during ascent, or (2): Crustal contamination (including post-magmatic alteration; Andersen, 1984). In the above discussion of Sr and Pb isochrons, a crustal contamination model was explicitly chosen. Although the present data do not justify an assumption of a unique and homogeneous isotopic signature within the mantle source region, the fact that the ascending magmas have penetrated a thick continental crust of early Proterozoic age, and that many samples show evidence of mechanical mixing with sand and the mineralogical effects of hydrothermal alteration (e.g. hydration and oxidation of mafic silicates, carbonatization of melilite) suggest that local contamination has obscured any evidence of mantle-derived heterogeneities in the Qassiarsuk magmatic system. This is further supported by the irregular variation of the initial isotopic characteristics within sample series taken from closely related rocks; see, for example, the considerable range of ε_{Nd} and ε_{Sr} for samples 30, 31 and 32, which come from a thin (2–3 m) unit of tuff SW of Qassiarsuk village (the 'sandy tuffisite' of

Stewart, 1970). Such patterns of isotopic variation are less easily explained by heterogeneities inherited from the mantle source than by variable extent of contamination with local crustal material.

Characterization of the end-member components

The crustal component. The granite composite, the fenite sample (48) and the two sandstone composites are uniform in terms of neodymium isotopic composition at 1.2 Ga, suggesting that the average local crust had an ε_{Nd} of *c.* −8. The strontium composition of the granitic gneiss and fenite, i.e. ε_{Sr} = *c.* 76, indicates the strontium isotopic composition of this reservoir, as the sandstone composites have suffered late-stage loss of radiogenic strontium. The two-stage lead evolution model suggests μ_1-values of 8.2 to 8.3 for the granitic gneiss and sandstone composites (Table 1), which is compatible with a moderately LILE-enriched continental crust of early Proterozoic age, and the best estimate of the U-Pb characteristics of the crustal reservoir. The position of this reservoir in the uranogenic lead correlation diagram at 1.2 Ga is indicated by ruling in Fig. 5*b*.

The mantle-derived component. Because contamination will shift initial Sr, Nd and Pb compositions towards the contaminant, only limiting estimates of the isotopic composition of the mantle-derived parent magma, and thereby of the mantle source, can be given from the present data. The maximum ε_{Nd} (+3.6) and minimum ε_{Sr} (−13) and μ_1 (7.4) define a minimum for ε_{Nd}, and maxima for ε_{Sr} and time-integrated $^{238}U/^{204}Pb$ for the mantle source. The permissible ranges for the Nd and Sr isotopic composition of the mantle source are compatible with previously published data on rocks of the Gardar rift (Blaxland *et al.*, 1978; Paslick *et al.*, 1993; Pearce and Leng, 1996). The position of the mantle source in the uranogenic lead diagram is illustrated by diagonal ruling in Fig. 5b. This low-μ_1 mantle signature differs significantly from the mantle source composition deduced for the *c.* 1.2 Ga Tugtutôq younger giant-dyke intrusion by Taylor and Upton (1993); it is, in fact, more similar to the least radiogenic leads observed in the Kûngnât Fjeld intrusion, which Taylor and Upton (1993) attributed to contamination with a LILE-depleted Archaean crustal component. The present lead isotopic data on the local crustal composites do not give any indications of the presence of depleted, Archaean material in the Qassiarsuk-Tasiusaq region, and the low μ_1 (< 7.7) therefore cannot be due to contamination, but must be a primary feature inherited from the mantle source. An evaluation of the consequences of these findings for the lead isotope systems of the Kûngnât Fjeld and Tugtutôq intrusions is beyond the scope of the present paper.

Contamination, differentiation and magmatic evolution

In plots of initial isotopic composition *vs.* inverse elemental concentration, bulk contamination (mixing) between isotopically distinct end-members, which affects both isotopic composition and trace element concentrations, shifts the compositions along straight lines connecting uncontaminated magma composition and the contaminant (Faure, 1986), e.g. along the black arrows in Fig. 6. On the other hand, magmatic differentiation processes (fractional crystallization, liquid immiscibility) will affect only the element concentrations, as indicated by the open arrows in Fig. 6. The range of strontium isotopic composition in the Qassiarsuk complex (Fig. 6*a*) can be fully explained by either mixing of batches of magma having different strontium concentrations with a uniform crustal end-member,

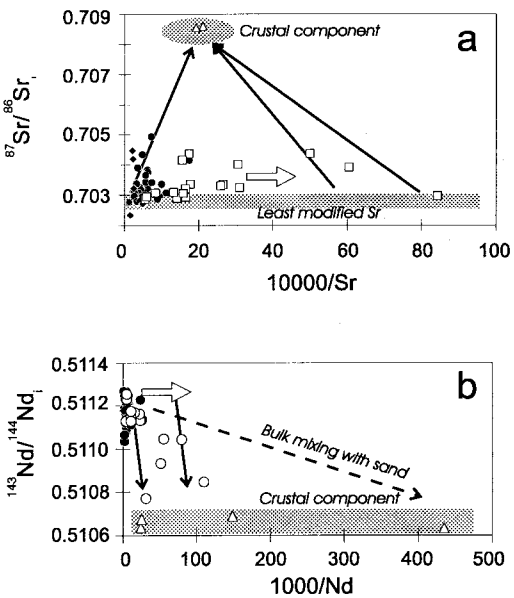

FIG. 6. The correlation between inverse Sr (*a*) and Nd (*b*) concentrations and recalculated isotopic composition at 1.2 Ga. The shaded fields reflect the ranges of composition for the different source regions represented in the Qassiarsuk complex. The solid arrows are possible two-component bulk mixing lines, the open arrows represent possible changes of trace element concentration brought about by closed-system magmatic differentiation processes. The broken arrow in *b* represents a possible contamination traject for a magma mixed with low-Nd sand during eruption. See the text for further discussion. Symbols as in Fig. 2

or by mixing between uniform mantle- and crustally derived components, followed by differentiation of different batches of contaminated melts. The same two mechanisms may account for the variation in the neodymium system (Fig. 6*b*). It should, however, be noted that bulk mixing between a magma and low-Nd sand apparently does not have a significant effect on the neodymium system (a hypothetical bulk contamination trend is shown as a broken arrow in Fig. 6*b*). This may be somewhat unexpected, given the presence of 'sandy' tuffs, which are thoroughly intermixed with local sand. The quartz-dominated sand is, however, too low in Nd to affect the isotopic composition of Nd in rocks with several tens of parts per million of Nd. The observed contamination trends in the Nd system must therefore have been formed before final emplacement of the diatremes or extrusion of the tuffs.

The Sr and Nd data do not define the relative timing of magmatic differentiation and contamination processes in the Qassiarsuk magmatic system. However, comparing the behaviour of lead and neodymium gives an answer to this question. Fig. 7 shows that the effects of contamination on the lead and neodymium systems in the Qassiarsuk complex are strongly decoupled from each other. As in the case of Sr and Nd (Fig. 6), the sensitivity of the lead system to contamination is dependent on concentration as well as isotopic composition; samples with elevated lead concentration are least sensitive to contamination of the lead system. The sample showing the least radiogenic lead isotopic composition and lowest μ_1 (sample 92/19), also has low Nd (32 ppm) and Sr (376 ppm) concentrations compared to other samples, and a low calculated μ_2-value. Sr and Nd are strongly contaminated, whereas the lead composition is unaffected. As well as indicating a low U-concentration, low μ_2 may indicate elevated Pb concentration, or a combination of both. The preservation of the lead mantle signature in 92 and the other low μ_1 samples, and the general lack of linear correlation between ε_{Nd} and μ_1 in Fig. 7 therefore indicates that magmatic differentiation had taken place before contamination with crustal material.

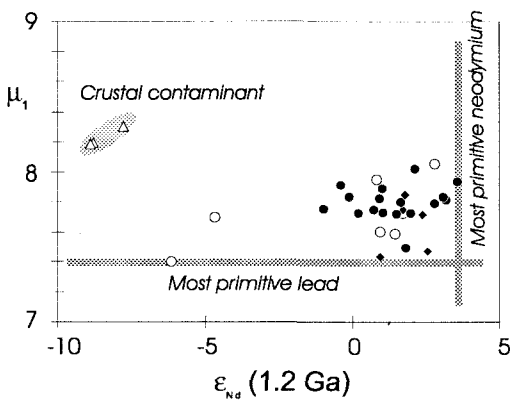

FIG. 7. Decoupling of the lead and neodymium isotopic systems in the Qassiarsuk complex. The shaded bars indicate the lowest μ_1 and highest ε_{Nd} seen in the Qassiarsuk complex, and represent the least contaminated magmas, defining minimum-depletion limits for the mantle source. Sample symbols as in Fig. 2.

Modelling of contamination trends

Strontium and neodymium. Fig. 8 shows Sr-Nd bulk contamination trends for the Qassiarsuk magmatic system at 1.2 Ga, assuming mixing of a depleted mantle derived component and the local crust, using a global depleted mantle end-member composition compatible with the limits derived above (Table 2). The two trends illustrated represent a 'carbonatite magma' composition (*a*), which is high in both Sr and Nd, and an 'alkaline mafic- to ultramafic magma' end-member (*b*), much lower in both elements. As can be seen, bulk contamination can account for the ranges in intitial Sr and Nd composition of the carbonatites and alkaline silicate rocks, but the amounts of crustal material required

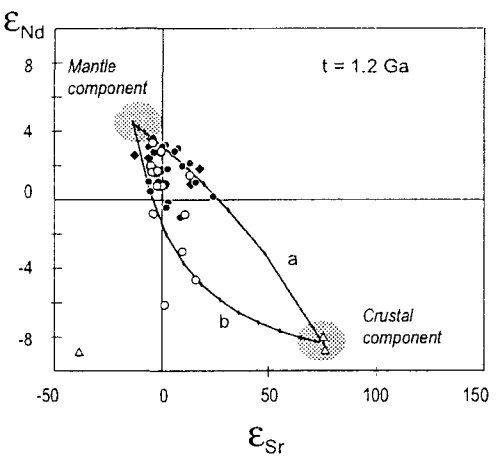

FIG. 8. ε_{Sr}–ε_{Nd} diagram for the Qassiarsuk rocks, with mixing curves calculated for typical mantle derived 'carbonatite' (*a*: high Sr, moderate Nd) and silicate (*b*: moderate Sr and low Nd) magmatic components and a local crustal component. The mixing-parameters are defined in Table 2. The mixing curves are marked at 10% intervals. Sample symbols as in Fig. 2.

TABLE 2. Mixing parameters

End-member	ppm Sr	ϵ_{Sr}	ppm Nd	ϵ_{Nd}	μ_1
Mantle-derived carbonatite magma	2000	−13.2	250	4.4	7.4
Mantle-derived mafic to ultramafic magma	600	−13.2	10	4.4	7.4
Pre-Gardar continental crust	500	76	10	−8.4	8.2

along the 'carbonatite trend' (30 to 70 percent by weight) may be too high to make bulk contamination a realistic process. An element-selective exchange process with the country-rocks during ascent is much more likely, perhaps acting in concert with bulk contamination. In the Fen complex, Norway, selective contamination of the strontium and lead systems was related to metasomatic alteration of feldspathic wallrocks along the magma conduit (Andersen, 1986, 1987), and further exchange with the country-rocks took place during post-magmatic hydrothermal alteration (Andersen, 1984, 1987). Clearly, both of these processes may have operated in the Qassiarsuk complex as well.

Lead. With the exception of the apparently contamination-resistant low-μ_1 samples, most carbonatites, apatite-enriched rocks and alkaline silicate rocks have μ_1-values in the range 7.7 to 7.9. Other carbonatite complexes show strong evidence of crustal influence on the initial lead isotopic composition (Fen: Andersen and Taylor, 1988; Alnö: Andersen, 1996*a*). Initial leads compatible with μ_1 = 7.7–7.9 can easily be produced by mixing a low-μ_1 mantle component (μ_1 = 7.4) with lead derived from the local crust (μ_1 = 8.2–8.3). For short time-differences, it is not possible to distinguish between the effects of contamination of a magma and early post-magmatic hydrothermal alteration (Andersen and Taylor, 1988). The preferred 1.2 Ga mantle source composition of Taylor and Upton (1993), shown as a star in Fig. 5b, coincides with the least radiogenic carbonatites and the μ_1 = 7.77 isochron from Qassiarsuk. As only samples below the isochron retain a reliable memory of the mantle source composition, this coincidence must be regarded as fortuitous.

Conclusions

The volcanic rocks exposed within the classical Qassiarsuk triangle of Stewart (1970) continue at least 2.5 km to the south and 7 kilometres westwards, to the north shore of Tasiusaq inlet, and possibly all the way to North Sermilik fjord. A main volcanic sequence, amounting to 40 m in thickness in the east gradually decreases to less than 10 m at the westernmost outcrops recognized in this study. This makes the Qassiarsuk volcanics a more volumetrically important feature of the Eriksfjord Formation than previously recognized. The volcanic rocks are over- and underlain by sandstones, and have been correlated with the Mussartût volcanic member. A series of carbonatitic diatremes in the underlying sandstones south and west of Qassiarsuk have probably acted as feeders for the extrusive carbonatites.

The volcanic rocks predate a dense swarm of Gardar dykes, striking N60°E, and faulting related to these dykes. Rb-Sr and Pb-Pb isochrons on carbonatites and alkaline silicate rocks give dates close to 1.2 Ga (1176 ± 8 Ma, whole-rock Pb-Pb, 1205 ± 12 Ma, Rb-Sr, whole rocks, 1234 ± 34 Ma, Rb-Sr on mica separates from lamprophyres), indistinguishable from the Nd mineral isochron ages (1.17–1.20 Ga) on the Ulukasik volcanic Member reported by Paslick *et al.* (1993). This suggests that the entire sequence of sedimentary and volcanic rocks of the Erikfsjord Formation was deposited within a comparatively short time period.

Carbonatite- and alkaline silicate magmas at Qassiarsuk have isotopic and trace element signatures indicating that they are comagmatic, derived from a CO_2-bearing, mafic mantle derived parent magma. The initial isotopic signature (at 1.2 Ga) of the carbonatites and alkaline silicate rocks suggests that the parent magma was derived from a LILE- and *LREE* depleted mantle source ($\epsilon_{Nd} > 4$, $\epsilon_{Sr} < -13$, $\mu \leqslant 7.4$), which may have been metasomatically enriched in CO_2 and other incompatible trace components prior to partial melting. The mantle-derived melts have gone through a stage of magmatic differentiation, forming carbonatitic and alkaline silicate magmas, which were later contaminated with local, pre-Gardar continental crust.

Whereas the Sr and Nd isotopic signatures of the mantle source are similar to what has been found in other studies of the Gardar igneous rocks (Blaxland *et al.*, 1978; Paslick *et al.*, 1993; Pearce and Leng, 1996), the very unradiogenic initial Pb isotopic composition seen in the least contaminated rocks

from Qassiarsuk ($^{206}Pb/^{204}Pb$ = 16.19, $^{207}Pb/^{204}Pb$ = 15.02) is compatible with a mantle source with μ_1 = 7.4, significantly less radiogenic than the mantle source inferred for the younger Tugtutôq giant dyke by Taylor and Upton (1993). The reason for this difference is unknown, but merits further research.

Acknowledgements

Economic support for field- and laboratory work from the Nansen Foundation is gratefully acknowledged. The Geological Survey of Denmark and Greenland (GEUS), Copenhagen, provided samples, and has authorized publication of the present paper. Special thanks are due to Lotte Melchior Larsen, GEUS, for discussions and support throughout the study. The author is grateful to Henning Sørensen and Brian Upton, who first introduced him to the Qassiarsuk complex, to Adrian P. Jones for suggesting a re-study of Qassiarsuk, for providing samples and for stimulating discussions, to Marion Seiersten for assistance in the field, to the Fredriksen family at Tasiusaq for hospitality, to Gunnborg Bye Fjeld, Toril Enger and Arne Stabel for analytical assistance, and to numerous friends and colleagues for helpful discussions and critical comments. Andy Chambers and Adrian Finch convened the Intraplate Alkaline Magmatism conference in Birmingham in April 1996, at which a preliminary account of this work was presented.

References

Allaart, J.H. (1983) *Geological map of Greenland, 1:100 000,. Narssarssuaq, 61V.3 Syd. Descriptive text*. Grønlands Geologiske Undersøgelse, Copenhagen, 20 pp.

Andersen, T. (1983) Iron ores in the Fen central complex, Telemark (S. Norway): Petrography, chemical evolution and conditions of equilibrium. *Norsk Geol. Tidsskr.*, **63,** 73–82.

Andersen, T. (1984) Secondary processes in carbonatites: petrology of 'rødberg' hematite-calcite-dolomite carbonatite) in the Fen central complex, Telemark (South Norway). *Lithos*, **17,** 227–45,

Andersen, T. (1986) Magmatic fluids in the Fen carbonatite complex, S.E. Norway. Evidence of mid-crustal fractionation from solid and fluid inclusions in apatite. *Contrib. Mineral. Petrol.*, **93,** 491–503.

Andersen, T. (1987) Mantle and crustal components in a carbonatite complex, and the evolution of carbonatite magma: REE and isotopic evidence from the Fen complex, S.E. Norway. *Chem. Geol., (Isotope Geosci. Sect.)*, **65,** 147–66.

Andersen, T. (1988) Evolution of peralkaline calcite carbonatite magma in the Fen complex, SE Norway. *Lithos*, **22,** 99–112.

Andersen, T. (1996*a*) Sr, Nd and Pb isotopic characteristics of the Alnö carbonatite complex, Sweden. *Abstracts, The 22nd Nordic Geological Winter Meeting, Turku, Finland,* 11.

Andersen, T. (1996*b*) Age and petogenesis of the Qassiarsuk carbonatite - alkaline silicate complex, South Greenland (abstract). *Intraplate Alkaline Magmatism, Birmingham, 1996.*

Andersen, T. and Munz, I.A. (1995) Radiogenic whole-rock lead in Precambrian metasedimentary gneisses from South Norway: Evidence for LILE mobility. *Norsk Geol. Tidsskr.* **75,** 156–68.

Andersen, T. and Sundvoll, B. (1986) Strontium and neodymium isotopic composition of an early tinguaite (nepheline microsyenite) in the Fen complex, S.E. Norway: Age and petrogenetic implications. *Norges geol. Unders. Bull.,* **409,** 29–34.

Andersen, T. and Taylor, P.N. (1988) Lead isotope geochemistry of the Fen carbonatite complex, S.E. Norway: Age and petrogenetic implications. *Geochim. Cosmochim. Acta*, **52,** 209–15.

Barker, D.S. (1989) Field relations of carbonatites. In *Carbonatites, Genesis and Evolution* (K. Bell, ed.). Unwin Hyman, London, 38–69.

Bell, K. and Blenkinsop, J. (1989) Neodymium and Strontium isotope geochemistry of carbonatites. In *Carbonatites, Genesis and Evolution* (K. Bell, ed.). Unwin Hyman, London, 278–300.

Blaxland, A.R., van Bremen, O., Emeleus, C.H. and Anderson, J.G. (1978) Age and origin of the major syenite centers in the Gardar province of South Greenland. *Geol. Soc. Amer. Bull.*, **89,** 231–44.

Boynton, W.V. (1984) Geochemistry of the rare earth elements: meteorite studies. In *Rare Earth Element Geochemistry* (P. Henderson, ed.), Elsevier, 63–114

Bruecner, H.K. and Rex, D.C. (1980) K-A and Rb-Sr geochronology and Sr isotopic study of the Alnö alkaline complex, northeastern Sweden. *Lithos,* **13,** 111–9.

Church, A.A. and Jones, A.P. (1995) Silicate-carbonate immiscibility at Oldoinyo Lengai. *J. Petrol.*, **96,** 869–89.

Dahlgren, S. (1987) *The satellitic intrusions in the Fen carbonatite alkaline rock province, Telemark, south-eastern Norway.* Unpublished Cand. Scient. Thesis, University of Oslo. 298 pp.

Dahlgren, S. (1993) Late Proterozoic and Carboniferous ultramafic magmatism of carbonatitic affinity in southern Norway. *Lithos,* **31,** 141–54.

Dawson, J.B. (1962) Sodium carbonate lavas from Oldoinyo Lengai, Tanganyika. *Nature,* **195,** 1075–6.

Dawson, J.B. (1989) Sodium carbonatite extrusions from Oldoinyo Lengai, Tanzania: implications for carbonatite complex genesis. In *Carbonatites, Genesis and Evolution* (K. Bell, ed.). Unwin

Hyman, London, 255–77.

DePaolo, D.J. (1981) Neodymium isotopes in the Colorado Front Range and crust-mantle evolution in the Proterozoic. *Nature,* **291,** 193–6.

Emeleus, C.H. and Upton, B.G. (1976) The Gardar Period in Southern Greenland. In *Geology of Greenland,* (A. Escher and W.S. Watt, eds.), Geological Survey of Greenland, Copenhagen, 152–81.

Faure, G. (1977) *Principles of Isotope Geology,* 1st edition. J. Wiley and Sons, New York. 464 pp.

Faure, G. (1986) *Principles of Isotope Geology,* 2nd edition. J. Wiley and Sons, New York. 589 pp.

Jahn, B.-m. and Cuvellier, H. (1994) Pb-Pb and U-Pb geochronology of carbonate rocks: an assessment. *Chem. Geol.,* 115, 125–51.

Kalsbeek, F., Larsen, L.M. and Bondam, J. (1990) *Geological map of Greenland, 1:500 000, Sydgrønland, sheet 1. Descriptive text.* Grønlands Geologiske Undersøgelse, Copenhagen.

Keller, J. (1989) Extrusive carbonatites and their significance. In *Carbonatites, Genesis and Evolution* (K. Bell, ed.). Unwin Hyman, London, 70–88.

Kjarsgaard, B.A. and Hamilton, D.L. (1988) Liquid immiscibility and the origin of alkali-poor carbonatite. *Mineral. Mag.,* **52,** 43–55.

Kjarsgaard, B.A. and Hamilton, D.L. (1989) The genesis of carbonatites. In *Carbonatites, Genesis and Evolution* (K. Bell, ed.). Unwin Hyman, London, pp. 388–404.

Knudsen, C. (1985) *Apatite mineralization in carbonatite and ultramafic intrusions in Greenland. Final Report.* Grønlands Geologiske Undersøgelse, Copenhagen, 176 pp.

Kwon, S.-T., Tilton, G.R. and Grünenfelder, M.H. (1989) Lead isotope relationships in carbonatites and alkalic complexes: an overview. In *Carbonatites, Genesis and Evolution* (K. Bell, ed.). Unwin Hyman, London, 360–387.

Le Bas, M.J. (1989) Diversification of carbonatite. In *Carbonatites, Genesis and Evolution* (K. Bell, ed.). Unwin Hyman, London, 428–47.

Ludwig, K.R. (1991) ISOPLOT; a plotting and regression program for radiogenic-isotope data; version 2.53. *U.S. Geol. Surv. Open File Report* **91–445,** 39 pp.

Paslick, C.R., Halliday, A.N., Davies, G.R., Mezger, K. and Upton, B.G. (1993) Timing of Proterozoic magmatism in the Gardar Province, Southern Greenland. *Geol. Soc. Amer. Bull.,* **105,** 272–8.

Pearce, N.J.G. and Leng, M.J. (1996) The origin of carbonatites and related rocks from the Igaliko Dyke swarm, Gardar Province, South Greenland: field, geochemical and C-O-Sr-Nd isotope evidence. *Lithos,* **39,** 21–40.

Peterson, T.D. (1989*a*) Peralkaline nephelinites. I. Comparative petrology of Shombole and Oldoinyo Lengai. *Contrib. Mineral. Petrol.,* **101,** 458–78.

Peterson, T.D. (1989*b*) Peralkaline nephelinites. 2 Low pressure fractionation and the hypersodic lavas of Oldoinyo Lengai. *Contrib. Mineral. Petrol.,* **102,** 336–46.

Peterson, T.D. (1990) Petrology and genesis of natrocarbonatite. *Contrib. Mineral. Petrol.,* **105,** 143–55.

Poulsen, V. (1964) The sandstsones of the Precambrian Eriksfjord formation in South Greenland. *Rapp. Grønlands geol. Unders.,* **2,** 16 pp.

Stewart, J.W. (1970) Precambrian alkaline-ultramafic/carbonatite volcanism at Qagssiarssuk, South Greenland. *Meddl. Grønland,* **186,** 4, 70 pp.

Tatsumoto, M., Knight, R.J. and Allègre, C.J. (1973) Time differences in the formation of meteorites as determined from the ratio of lead 207 to lead 206. *Science,* **180,** 1279–83.

Taylor, P. N. and Upton, B.G. (1993) Contrasting Pb isotopic compositions in two intrusive complexes of the Gardar Magmatic Province of South Greenland. *Chem. Geol.,* **104,** 261–8.

Todt , W., Cliff, R.A., Hanser, A. and Hofmann, A.W. (1984) $^{202}Pb + {}^{205}Pb$ double spike for lead isotopic analyses (abstract). *Terra Cognita,* **4,** 209.

Verschure, R.H., Maijer, C., Andriessen, P.A.M., Boelrijk, N.A.I.M., Hebeda, E.H., Priem, N.H.A. and Verdurmen, E.A.T. (1983) Dating explosive volcanism perforating the Precambrian basement in Southern Norway. *Nor. geol. unders.,* **380,** 35–49.

Whitehouse, M.J. (1989) Pb-isotope evidence for U-Th-Pb behaviour in a prograde amphibolite to granulite facies transition from the Lewisian complex of north-west Scotland: Implications for Pb-Pb dating. *Geochim. Cosmoch. Acta,* **53,** 717–24.

[*Revised manuscript received 18 February 1997*]